

SWEENEY CONVENTION CENTER / SANTA FE / NEW MEXICO  
3 - 5 JUNE 1992

# Rock Mechanics Proceedings of the 33rd U.S. Symposium

*Edited by*

J.R. TILLERSON & W.R. WAWERSIK

*Sandia National Laboratories, Santa Fe*

OFFPRINT



A.A. BALKEMA / ROTTERDAM / BROOKFIELD / 1992

# Reservoir compaction and surface subsidence above the Lost Hills Field, California

M.S. Bruno & C.A. Boyberg

*Chevron Oil Field Research Co., La Habra, Calif., USA*

**ABSTRACT:** Reservoir compaction and surface subsidence have been associated with oil and gas production from several diatomite reservoirs in the San Joaquin Valley, California, during the past 40 years. These reservoirs are characterized by relatively soft and porous formation material, and relatively shallow and thick producing intervals. Surface subsidence above some of these oil fields is often significant and costly, sometimes exceeding a foot per year and inducing damage to hundreds of wells. In order to support expanded development at the Lost Hills Field, Chevron initiated in 1989 an extensive program of rock properties measurements in the laboratory, analytical and numerical modelling efforts, and field observations of subsurface compaction and surface subsidence. This paper presents some initial results of these ongoing analyses and measurements.

## 1 INTRODUCTION

The Lost Hills Oil Field is located along the west side of the San Joaquin Valley about 40 miles northwest of Bakersfield, California. A cross section and partial contour map at the top of the diatomite interval are presented in Figures 1 and 2. The producing structure is one of several elongate, asymmetric anticlines trending NW-SE which developed in response to later Tertiary compression and translation associated with the San Andreas Fault system. Other major fields include Belridge, Buena Vista, and Midway-Sunset. Much of the production from these reservoirs comes from soft, thick beds of diatomite and mudstone, which range in depth from about 1000 feet to 2400. The formation material is often characterized by very high porosity (to 60%), high oil saturation (to 60%), and low matrix permeability (0.1 to 5 md). The diatomite may be naturally fractured, but not extensively, and generally requires massive hydraulic fracture stimulation to support economic oil production.

Because the producing formations are relatively soft, thick, and shallow, reservoir compaction and surface subsidence have been associated with oil and gas production from several diatomite reservoirs in the area during the past 40 years. In the most extreme example, portions of the Belridge Field subsided more than 9 feet during the mid-1980s, resulting in damage to more than 400 wells operated by several oil companies. The surface above the Lost Hills Field has been subsiding since the early 1950's, and has recently accelerated due to expanded well development in the late 1980's.

## 2 COMPACTION AND SUBSIDENCE FIELD OBSERVATIONS

Before 1980 the rate of surface local surface subsidence above the Lost Hills was on the order of tenths of inches per year. The effects of oil and gas production on surface subsidence was insignificant compared to the effects of ground water withdrawal for

agriculture throughout the San Joaquin Valley, which caused some areas to subside as much as 30 feet from 1925 to 1977 (see Poland and Davis, 1969). Additional field development in the mid to late 1980's have increased local subsidence at Lost Hills to the current rate of about 1 ft/year.

Since 1989 Global Positioning Satellite (GPS) surveys have been conducted quarterly at approximately 70 monument locations spread over the surface of the Lost Hills Field. Figure 3 presents a contour plot of subsidence above the Lost Hills Field from January, 1989 through April, 1991. During this period subsidence has been almost linearly related to total fluid production from the center of the field. Subsurface formation compaction has been measured with less precision through the use of radioactive bullet logs in one well and gamma logs of natural markers in other wells. Preliminary measurements suggest the diatomite interval compacted about 2 ft from 1990 to 1991.

### 3. LOST HILLS FIELD LITHOLOGY

The Lost Hills Field is a northwest-southeast doubly plunging anticline, about 8 miles long and 1 mile wide, that produces both light and heavy oil. The distribution of high oil saturation and porosity zones, however, generally confine production to the southeastern half of the structure. The crest plunges at dips of 2-4 degrees, and the flanks dip as high as 25 degrees. A section cutting SW-NE across the structure is presented in Figure 1. The primary formation materials include sands and gravel of the shallow Tulare Formation, siltstones, shales and thin sand strings of the San Joaquin Formation and Etchegoin Formations, the Belridge Diatomite of the upper Reef Ridge Formation, and the siliceous shales of the lower Reef Ridge and Mclure Formations.

#### 3.1 Tulare Formation Sands

The sediments of the Tulare Formation include thin-bedded clay, silt, fine-grained sandstone, and limestone which are interpreted as lacustrine deposits, and cross-bedded silty and pebbly sandstone and conglomerate that are interpreted as fluvial deposits (Chiou, et. al., 1990). This commingled depositional environment yields a high proportion of shale barriers, with lateral continuity of the sands rarely greater than 500 feet. The Tulare sands tend to be finer grained than the Etchegoin, but possess similar permeabilities and porosities. Some residual heavy oil from a relict oil-water contact is produced by steam in the northern area of Lost Hills Field. Rock properties from routine core analysis show that the higher quality sands have an oil saturation (12 degree API) of about 60%, porosity of 38%, and permeability of 5 md.

#### 3.2 San Joaquin Formation Siltstone

The Pliocene San Joaquin Formation siltstone is a member of the Etchegoin Group (Loomis, 1990) which records a regressive sequence of clastic dominated sediments. The San Joaquin Formation is composed of a basal conglomerate member and overlying undifferentiated sandstone, siltstone, and claystone. The lithologies overlying the conglomerate member are predominantly silty, including laminated gray and rust-brown claystone, siltstone, and very fine-grained sandstone (Loomis, 1990). The San Joaquin Formation in the Lost Hills Field varies in thickness from about 600 ft. at the anticlinal crest to zero thickness along most of the flanks.

The rock properties of the upper interval of the San Joaquin Formation siltstone were measured on vertical core plug samples obtained in 1990. Radioactive bullets were shot into the formation for subsequent monitoring of rock compaction. The rock can be classified as a gray diatomaceous feldspathic siltstone. The components are: 30% clay minerals, 50% silt-sized framework minerals, 5% biogenic silica, 7% siderite and dolomite, and 4% organics. The framework minerals are predominantly plagioclase

feldspar grains (90%), with minor amounts of quartz (5%), micas (3%), and lithic fragments (2%). The clay matrix is predominated by smectite (15%), with lesser amounts of illite (7%) and kaolinite (7%). The rock porosity varies from 40 to 50%.

### 3.3 The Belridge Diatomite

The Belridge diatomite is the uppermost unit of the late Miocene to early Pliocene Reef Ridge Shale Member of the Monterey Formation and is unconformably overlain by the middle Pliocene Etchegoin Group. The Reef Ridge Shale conformably overlays the Antelope and McDonald Units of the McLure Member of the Monterey Formation (Graham and Williams, 1985). The biogenic silica of Reef Ridge shale is of the opal-A composition and the McLure Member are opal-CT (crystobalite-tridymite) to quartz in composition. The Reef Ridge Shale records basin filling and shallowing, with encroachment of siliciclastic depositional systems. It consists largely of siliceous shales and clay shales, becoming less siliceous and sandier upward.

The major producing interval at Lost Hills Field is the opal-A Belridge diatomite. A structural contour from this interval is presented in Figure 2. A pressure and temperature dependent mineralogical phase change from opal-A to CT occurs at a crestal depth of about 2100 feet and generally limits matrix controlled production to depths shallower than this. Within this phase change spectrum from opal-A through quartz, there occurs a porosity decline from about 65% to 35% and a density increase from about 1.5 gm/cc to 2.65 g/cc. The Belridge diatomite compositionally consists of subequal amounts of sand and silt, clays and biogenic silica. A scanning electron microscope (SEM) photo is presented in Figure 3. Stratigraphically, the Belridge diatomite shows a pronounced coarsening upwards with basal argillaceous diatomites, gradually giving way to diatomaceous siltstones and sandstones.

### 3.4 Lower Reef Ridge and McLure Formation Shales

The Lower Reef Ridge and McLure Formation is characterized by abundant porcellanites and siliceous shales, with silica occurring as diagenetic opal-CT and quartz. The top of the McLure Formation marks the end of the predominantly biogenic sedimentation due to encroachment of basin-margin clastics (Graham and Williams, 1985). The gray-brown porcellaneous interval (Antelope Unit) is comprised of porcellanite or porcellaneous shale and mudstone that is blocky in bedding, brittle and well-indurated. This interval contains the phase transition from Opal-A to Opal-CT. The rock is generally hard and denser than diatomite. The siliceous shale interval may be comprised of approximately 50% clay minerals and 50% diagenetic and detrital quartz. The siliceous shale interval (McDonald Unit) is less brittle, generally thinly-bedded and often fissile. Opal-CT comprises approximately 90% of the rock, with diatom frustules rarely recognizable. Other mineral components are feldspars, pyrite, siderite, mica, quartz, and calcite.

The thickness of the McLure Formation in the Lost Hills Field is approximately 220 feet of the Antelope unit and 180 feet of the McDonald unit. Rock properties were measured on core samples from Well CAHN 8-11C for the depth interval of 4500 to 4900 feet. The porosity averages approximately 38%, and permeability of less than 1.0 md. Matrix permeability and porosity are reduced significantly from the opal-A to the quartz. Limited reservoir production is facilitated by natural and induced fractures.

## 4. ROCK MECHANICAL PROPERTIES

The weight of sediments overlaying a producing formation is supported partially by the rock matrix and partially by the fluid pressure in the rock pores. When the reservoir fluid pressure is depleted, more of the load is transferred to the rock matrix and the formation

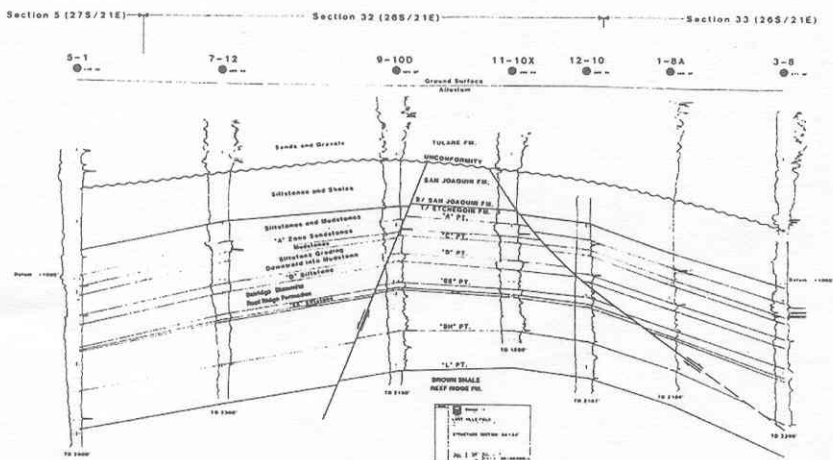


Figure 1. Lost Hills Reservoir SW-NE Trending Cross Section

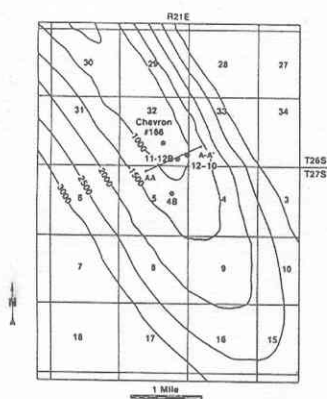


Figure 2. Structure Contour Map, Top of Diatomite Over the South-Central Lost Hills Reservoir

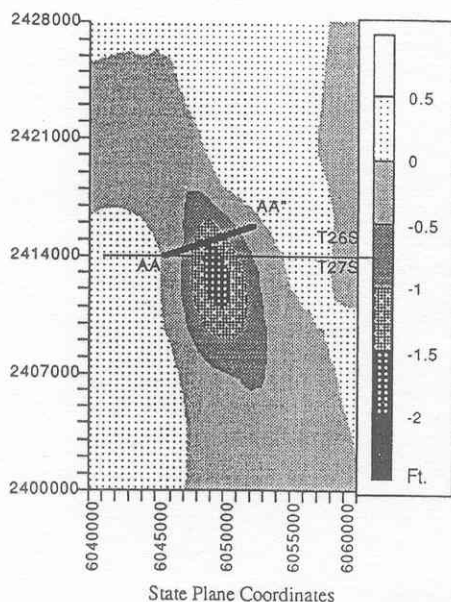


Figure 3. Lost Hills Surface Subsidence. Elevation Change from 1/89 to 4/91

volume compacts. The primary control on this formation compaction is therefore influenced by the material pore volume compressibility  $C_p$  and bulk compressibility  $C_b$  defined as the change in pore volume  $V_p$  and bulk volume  $V_b$  with respect to pore pressure  $P_p$  at constant confining pressure:

$$(1) \quad C_p = \frac{1}{V_p} \left( \frac{\partial V_p}{\partial P_p} \right) ; \quad C_b = \frac{1}{V_b} \left( \frac{\partial V_b}{\partial P_p} \right)$$

While in theory the pore and bulk volume compressibilities are physically well defined and may be related to other compressibility measures and elastic constants (see Zimmerman et. al., 1986), in fact diatomite deforms inelastically at almost all stress levels and reported compressibility values are simply empirical measures of volume change subject to some laboratory imposed stress conditions. A typical practice is to assume an effective stress law is valid and to measure compressibility with respect to changes in confining pressure under fully drained conditions.

#### 4.1 Diatomite

A relatively small number of investigations into the mechanical properties of diatomite have been reported in the literature. Stosur and David (1976) describe tests conducted on Lost Hills Opal A samples which show slightly increased compressibility when effective stresses exceeded 1000 to 1100 psi. They attributed increased compressibility to possible crushing of diatoms, with greater compressibility changes associated with higher diatom concentration. Pore volume compressibility for these samples was on the order of 50E-6/psi.

Strickland (1985) presents dynamic and static mechanical properties on a single sample of Opal A diatomite from Belridge. At low confining pressure the static and dynamic Young's modulus are reported in the range of 3.2 to 3.6 E-5 psi and Poisson's ratio on the order of 0.16. For this sample, plastic deformation accelerated above a mean stress level of about 1000 psi, and the Young's modulus was reduced by a about a factor of two. For a material of 50% porosity, these stiffness properties would correspond to pore volume compressibility values of about 25 E-6 psi. Wendel et. al. (1988) report pore volume compressibility on oil saturated diatomite samples on the order of 60 E-6 psi. and Bowersox (1990) reports compressibility values on brine saturated samples on the order of 160 E-6 psi. This range in reported compressibility values (from about 20 to 200 E-6 psi) is not unreasonable for diatomite considering the large variability in mineralogy and porosity of various samples.

To further evaluate Lost Hills Diatomite material properties, triaxial stress tests were conducted on Opal A core samples from a depth of about 2100 feet in sections 4 and 32. Cylindrical samples, 2.12in diameter and from 4 to 5 inches in length were cut perpendicular to bedding and enclosed in a teflon sleeve. The samples were not cleaned or dried to avoid strength alteration due to fluid chemistry. For some tests, pore pressure and confining pressure were held constant and axial load was increased until failure. Strains were measured with three axial and three radial LVDTs. Fluid expelled was also monitored. Axial load was applied at a strain rate of 10E-6/sec. A typical stress-strain curve is presented in Figure 4, for a confining pressure of 250 psi and a pore pressure of 150 psi. The bulk compressibility for 3 samples from a well in Section 4 ranged from 18 to 30E-06/psi at an effective mean stress level of about 800 psi. The pore volume compressibility ranged from 30 to 70E-06/psi. Poisson's ratio averaged 0.20.

Other samples were subjected to hydrostatic compression at constant pore pressure. Figure 5 presents the loading and unloading path for one typical sample. The slope of bulk volume strain versus hydrostatic stress provides a measure of bulk compressibility. For this sample the compressibility is about 25E-6/psi at low confining stress. It increases to about 90E-6/psi as the material compacts and suffers microstructural damage, and then decreases slightly with further compaction. The material remains stiff during unloading,



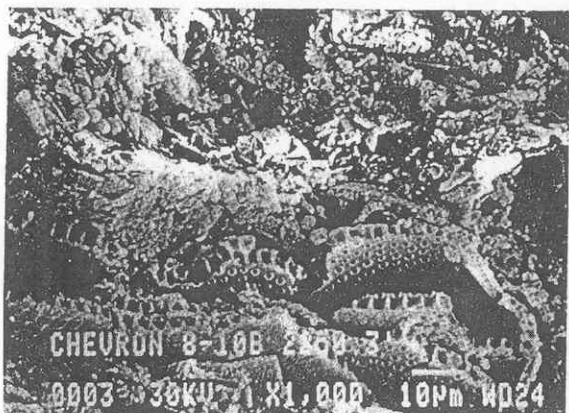


Figure 4. Diatomite SEM

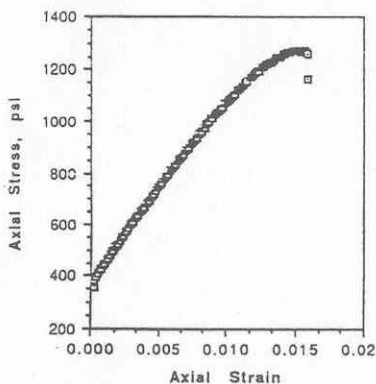


Figure 5. Diatomite Stress-Strain Curve

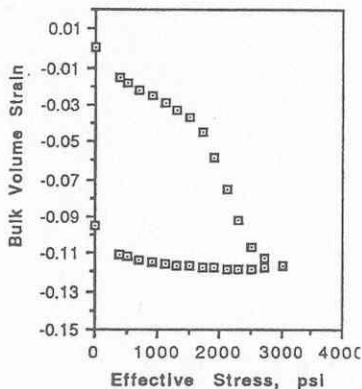


Figure 6. Diatomite Compressibility Example

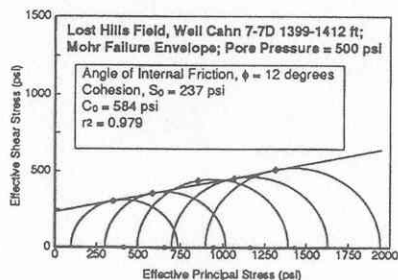


Figure 7. Lost Hills Siltstone Material Failure Envelope

clearly demonstrating irreversible damage and deformation. This stiffer unloading behavior has implications for water injections strategies required to control future subsidence. The pore volume compressibility measured by a commercial lab for three additional samples taken from Section 33 at the same depth interval (about 2000 feet) ranged from 25 to 45E-06/psi. These tests also demonstrated an increased compressibility as effective stresses exceeded about 1200 psi.

## 4.2 Overburden Material

The degree to which subsurface formation compaction induces surface subsidence is controlled by the reservoir geometry and the stiffness properties of the material surrounding the pressure depleted zone, both within the producing formation and the overburden material. Subsidence-induced well damage often occurs above the producing interval due to shear deformation, fault movement, or bedding plane slip (Bruno, 1992). The overburden material properties must therefore be evaluated to accurately assess the influence of formation compaction on surface subsidence and possible well failure.

Five core samples from the San Joaquin Siltstone Formation overlaying the diatomite at Lost Hills were tested under triaxial stress conditions to determine stiffness and failure properties. Pore pressure and confining pressure were held constant, while axial load was increased until failure. This was repeated at several confining pressures in order to define a Mohr-Coulomb failure envelope, as shown in Figure 7. The average Young's Modulus measured 1.4E05 psi and the average Poisson's ratio was 0.30.

## 5 NUMERICAL MODEL

A finite element procedure (ADINA, 1988) has been applied to estimate surface subsidence and to qualitatively assess the potential for well casing damage. As discussed in section 3, material properties for the diatomite and overburden vary with lithology and location within the reservoir. Porosity and permeability throughout the field is also non-homogeneous, so that a number of simplifying assumptions are required. The Lost Hills Field is very long and narrow (about 8:1 ratio), with extensive well development along its length and width. It was therefore determined to model the field with a line of symmetry trending roughly N40W along its length. Subsequent field measurements of subsidence confirmed this approximate field symmetry (see figure 3).

A geologic cross section across a portion of the field and the corresponding finite element model are shown in Figure 8. The model is composed of 1581 nodal points defining 375 9-node elements. The entire geologic model extends to a depth of 6000 feet and to a half-width of 10000 feet. The producing diatomite interval occupies the center portion from a depth of 1200 feet to 2100 feet, with a half-width of 2000 feet. Nodal point spacing in the center portion of the field is every 120 feet.

The model includes four distinct materials, representing the sands and gravels of the Tulare Formation (Upper Sands), the siltstones and shales of the San Joaquin and upper Etchegoin Formation (Siltstones), the Opal A diatomite of the upper Reef Ridge Formation (Diatomite), and the Opal CT and shale material of the lower Reef Ridge and McLure Formations (Shale). Typical material properties for each of these lithologies are summarized in Table 1. It is important to keep in mind, however, that there is a wide range of variability for many of these properties.

Uncertainty in material property data is usually matched, if not exceeded, by uncertainty in fluid production and reservoir pressure data for most oil and gas reservoirs. The purpose of the numerical model is not to provide a precise prediction of future subsidence, but rather to qualitatively assess the potential for well damage and optimum injection strategies for future waterflooding. With this model there is no formal coupling between the fluid flow geomechanics problem. Deformations are directly related to an assumed pressure distribution, which in practice may be obtained from reservoir simulation or field production and pressure data.



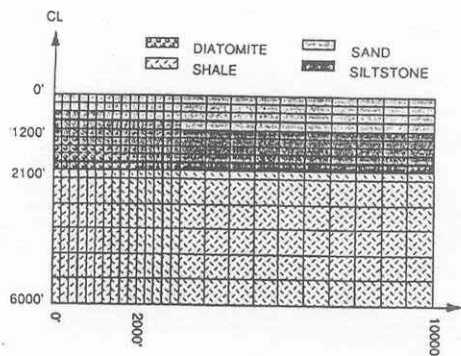


Figure 8. Lost Hills Finite Element Cross Section Model

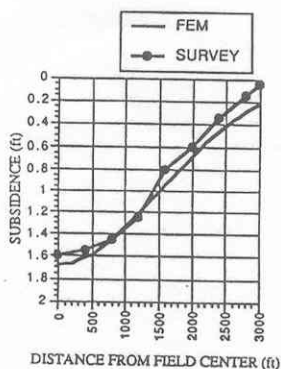


Figure 9. Comparison of Model and Field Measurements from 1/89 to 8/91

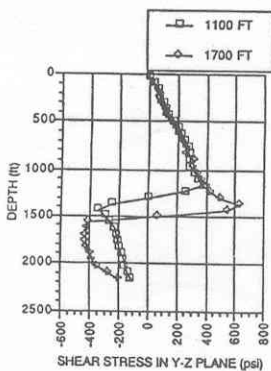


Figure 10. Shear Stress Profile at 1100 and 1700 ft from Reservoir Center (DP=700psi)

## 5.1 Material Models

The model has been used to investigate subsidence and overburden shear stresses induced by various possible pressure depletion scenarios. For a monotonic decrease in reservoir pore pressure, diatomite compressibility is assumed to vary with effective pressure according to the following relation:

$$(2) \quad \frac{\Delta V_b}{V_b} = C_{bo}(\Delta p + \beta \Delta p^2)$$

where, for example,  $C_{bo}=25E-6/\text{psi}$  and  $\beta=2.0E-3/\text{psi}$  for material data presented in figure 5 over an effective stress range from about 1000psi to 2000psi.

The shale formation lying beneath the diatomite zone is modeled as an elastic material. The overlying siltstone and sand layers are modeled with an elastic-perfectly-plastic constitutive relation and a Drucker-Prager yield condition (Bathe, 1982). Yielding is defined to occur when

$$(3) \quad \alpha \sigma_{kk} + \sqrt{\frac{1}{2} S_{ij} S_{ij}} - k = 0 ; \quad S_{ij} = \sigma_{ij} - \frac{1}{3} \delta_{ij} \sigma_{kk}$$

where:

$$(4) \quad \alpha = \frac{2 \sin \phi}{(3 - \sin \phi) \sqrt{3}} \quad k = \frac{6 S_0 \cos \phi}{(3 - \sin \phi) \sqrt{3}}$$

In the expressions listed above,  $\phi$  represents the friction angle for the material and  $S_0$  is the cohesion, or inherent shear strength. A summary of material properties used for the model is presented in Table 1.

Table 1: Formation Material Properties

Material	Young's Modulus (psi)	Poisson's Ratio $\nu$	Cohesion $S_0$ (psi)	Friction Angle $\phi$ (degrees)
Upper Sands	1.0 E05	0.20	50	30
Siltstones	1.4 E05	0.25	235	12
Diatomite	1.0 E05	0.25	400	15
Shale	5.0 E05	0.25	-	-

## 5.2 Comparison with Field Observations

Fieldwide pressure data for the Lost Hills field has not been generally available, so that a number of assumptions are required to compare model results with field data. A few pressure buildup well tests were conducted from 1988 through 1990. More extensive pressure monitoring has been underway since early 1991 in the Southwest corner of section 32. Based on this limited data, a qualitative estimate is that average reservoir pressure has declined by about 50psi/year since 1989. This is also generally consistent with reservoir simulations which have been adjusted to match historical production data.

Figure 9 presents a comparison of model results and field measurements above the studied cross section for the period from January, 1989 through August, 1991. The model results are based on the material properties presented in Table 1 and a uniform average pressure decline of 50 psi/year. The match is reasonable, although field data indicates less lateral spreading of the subsidence bowl than the numerical model.

The model results have also been used to indicate zones for potential well damage associated with overburden material shear failure, bedding plane slip, and possible fault movement. Figure 10 presents the induced shear stress profile with depth and lateral position above the studied cross section for a reservoir pressure decline. Large shear stresses are developed in the overburden material above the producing interval and towards the flanks of the reservoir. These locations for failure are consistent with casing damage at both Belridge and Lost Hills. In fact, shear-induced casing damage in the overburden or top of the producing interval has been a dominant failure mechanism in several subsiding reservoirs (Bruno, 1992).

A stress analysis such as shown in Figure 10, however, can only be used as a qualitative tool. These are only the additional stresses induced by production, and do not include in-situ stresses. Because the material behaves inelastically, these stresses cannot be simply superimposed. The maximum horizontal stress in the San Joaquin Valley trends approximately perpendicular to the San Andreas Fault and generally exceeds the vertical stress at depths above 2000 feet (Hansen and Purcell, 1986). This would tend to apply additional shear stresses at shallower depth and move the potential failure zone higher. A more detailed analysis including measured in-situ stresses and fluid flow coupling is continuing.

## REFERENCES

- ADINA Engineering Inc. 1984. ADINA theory and modeling guide. Report AE 84-4: Watertown, MA.
- Bathe, K.J. 1982. Finite element procedures in engineering analysis. Englewood Cliffs, New Jersey: Prentice-Hall, Inc.
- Bowersox, J.R. & R.A. Shore 1990. Reservoir compaction of the Belridge diatomite and surface subsidence, South Belridge Field, Kern County, California, in Kuespert, S.E. & S.A. Reid, eds., Structure, stratigraphy, and hydrocarbon occurrences of the San Joaquin Basin, California. Pacific Section SEPM, vol. 64: 225-230.
- Bruno, M.S. 1992. Subsidence-Induced Well Failure. SPE Drilling Engineering vol. 7, no. 1, SPE 20058.
- Chiou, R.C.S., T.L. Kirst, & C.W. Kiven 1990. Reservoir description and steamflood development in the Lost Hills Field: Society of Petroleum Engineers preprint no. 20727.
- Graham, S.A., and L.A. Williams 1985. Tectonic, depositional, and diagenetic history of Monterey Formation (Miocene), central San Joaquin basin, California. AAPG Bulletin, vol. 69: 385-411.
- Hansen K.S. & W.R. Purcell 1986. Earth Stress Measurements in the South Belridge Oil Field, Kern County, California, SPE 15641, 61st SPE Conf. New Orleans, Oct., 1986.
- Loomis, K.L. 1990. Depositional environments and sedimentary history of the Etchegoin Group, West-Central San Joaquin Valley, California, in Kuespert, S.E. & S.A. Reid, eds., Structure, stratigraphy, and hydrocarbon occurrences of the San Joaquin Basin, California. Pacific Section SEPM, vol. 64: 231-246.
- Poland J.F. & G.H. Davis 1969. Land subsidence due to fluid withdrawal, in: Reviews in Engineering Geology, Vol II. Geological Society of America, Boulder, Colorado
- Stosur, J.J. & A. David 1976. Petrophysical evaluation of the diatomite formation of the Lost Hills Field, California. Journal of Petroleum Technology vol. 28, October 1976: 1138-1144
- Strickland, F.G. 1985. Reasons for production decline in the diatomite, Belridge Oil Field: a rock mechanics view. Journal of Petroleum Technology vol. 37, March 1985: 521-526.
- Wendel, D.J., L.A. Kunkel, & G.S. Swanson 1988. Waterflood potential of diatomite: new laboratory methods, SPE 17439.
- Zimmerman, R.W., W.H. Somerton, & M.S. King 1986. Compressibility of porous rocks. Journal of Geophysical Research, vol. 91, no. B12: 12765-12777.